

T.C.
YEDİTEPE UNIVERSITY
INSTITUTE OF HEALTH SCIENCES
MEDICAL PHYSICS DEPARTMENT

**DOSIMETRIC CALCULATIONS IN ⁹⁰Y
MICROSPHERE TREATMENT**

GAMZE ERGİYEN BULDU

MASTER OF MEDICAL PHYSICS THESIS


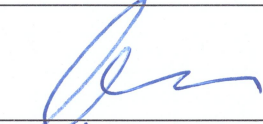
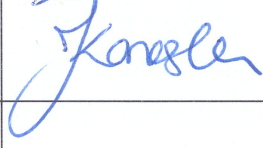
SUPERVISOR
DOÇ. DR. NALAN ALAN SELÇUK

İSTANBUL – 2019

TEZ ONAYI FORMU

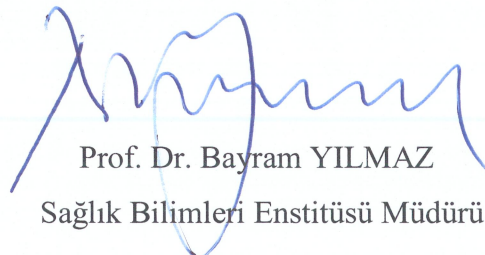
Kurum : Yeditepe Üniversitesi Sağlık Bilimleri Enstitüsü
Program : Sağlık Fiziği
Tez Başlığı : Dosimetric Calculations in ⁹⁰Y Microsphere Treatment
Tez Sahibi : Gamze Ergiyen Buldu
Sınav Tarihi : 16.12.2019

Bu çalışma jürimiz tarafından kapsam ve kalite yönünden Yüksek Lisans Tezi olarak kabul edilmiştir.

	Unvanı, Adı-Soyadı (Kurumu)	İmza
Jüri Başkanı:	Doç. Dr. Hatem Hakan Selçuk	
Tez danışmanı:	Doç. Dr. Nalan Alan Selçuk	
Üye:	Prof. Dr. İpek Karaaslan	
Üye:		
Üye:		

ONAY

Bu tez Yeditepe Üniversitesi Lisansüstü Eğitim-Öğretim ve Sınav Yönetmeliğinin ilgili maddeleri uyarınca yukarıdaki jüri tarafından uygun görülmüş ve Enstitü Yönetim Kurulu'nun 31./12./2019 tarih ve 2019/20-39 sayılı kararı ile onaylanmıştır.


Prof. Dr. Bayram YILMAZ
Sağlık Bilimleri Enstitüsü Müdürü

DECLARATION

I hereby declare that this thesis is my own work and that, to the best of my knowledge and belief, it contains no material previously published or written by another person nor material which has been accepted for the award of any other degree except where due acknowledgment has been made in the text.

Date 16.01.20

Signature

Name Surname

Ganze Egriyen Buldu



ACKNOWLEDGMENT

With all the effort made and attention paid this thesis work has been such a devotion to me and my dedicated supervisor Associate Professor Nalan Alan Selçuk. I thank my teachers Dr. Türkay Toklu and Prof. Dr. İpek Karaaslan for their help during my study. A special thank to my friend Seval Beykan who helped me and patiently answered all my questions whenever I needed. I also thank my husband Bulut and my family for their support.

TABLE OF CONTENTS

APPROVAL	ii
DECLARATION	iii
ACKNOWLEDGEMENTS	iv
TABLE of CONTENTS	v
LIST OF TABLES	viii
LIST OF FIGURES	ix
LIST OF SYMBOLS AND ABBREVIATIONS	x
ABSTRACT	xi
ABSTRACT (Turkish)	xii
1. INTRODUCTION and PURPOSE	1
2. LITERATURE REVIEW	2
2.1. Yttrium-90 Physical Properties	2
2.1.1. Bremsstrahlung Radiation	2
2.2. ⁹⁰ Y Microspheres	3
2.3. ⁹⁰ Y Glass Microspheres	3
2.4. ⁹⁰ Y Microspheres Treatment Procedure and Dosimetry	4
2.4.1. Administration of ⁹⁰ Y microsphere	4
2.5. Patient Selection of ⁹⁰ Y Microsphere Treatment	4
2.6. Before ⁹⁰ Y Microsphere Treatment	4
2.7. Dosimetric Calculations	7
2.7.1. Empirical Methods	7
2.7.2. Dosimetric Methods	8
2.7.2.1. Non-compartmental MIRD macro dosimetry	8
2.7.2.2. Compartmental MIRD Macro dosimetry	10
	v

2.7.2.3. Dosimetry at the voxel level	10
2.8. Reference Values	11
2.9. Radionuclide Imaging	12
2.9.1. Gama Camera	12
2.9.2. Spect/Ct	13
2.9.3. Pet/Ct	14
3. MATERIALS AND METHODS	16
3.1. Patient	16
3.2. ^{90}Y Microsphere Treatment Algorihtm	17
3.3. Patient Selection for ^{90}Y microsphere treatment	17
3.4. Tumor mapping – Angiography	18
3.5. $^{99\text{m}}$ TC-MAA Spect/Ct Imaging	18
3.6. Dose Calculation and Planing Volume Determination	19
3.7. ^{90}Y Pet/Ct Imaging	20
3.8. Bland Altmann Analysis	21
4. RESULTS AND DISCUSSION	22
4.1. Treatment Activities	22
4.2. Lung shunt fractions and lung doses	23
4.3. Absorbed doses for each patient based on $^{99\text{m}}\text{Tc}$ -MAA SPET/CT images	24
4.4. Absorbed doses for each patient based on on ^{90}Y PET/CT images	25
4.5. Tumor Absorbed Doses	26
4.6. Parenchyma Absorbed Doses	29
4.7. Liver Absorbed Doses	32
5. CONCLUSION	36

6. REFERENCES	37
7. ETHICS COMMITTEE REPORT	42
8. CV	43

LIST OF TABLES

Table 2.1. Recommended activity for tumor burden	7
Table 2.2. Tolerance limits for ^{90}Y microsphere treatment	12
Table 3.1. Specific characteristics of patients	16
Table 4.1. Required injected treatment activities for each patient based on $^{99\text{m}}\text{Tc}$ -MAA SPECT/CT images.	22
Table 4.2. Lung Shunt Fraction and Lung Dose value of patients	23
Table 4.3. Absorbed doses for each patient based on ^{90}Y PET/CT images	24
Table 4.4. Absorbed doses for each patient based on $^{99\text{m}}\text{Tc}$ -MAA SPET/CT images	25
Table 4.5. Tumor doses of pre-post dosimetry	26
Table 4.6. Results of Tumor Absorbed Doses Sample Statistics	27
Table 4.7. Results of Tumor Absorbed Doses one-sample T test	28
Table 4.8. Parenchyma doses of pre-post dosimetry	29
Table 4.9. Results of Parenchyma Absorbed Doses Sample Statistics	30
Table 4.10. Results of Parenchyma Absorbed Doses one-sample T test	31
Table 4.11. Liver doses of pre-post dosimetry	32
Table 4.12. Results of Liver Absorbed Doses Sample Statistics	33
Table 4.13. Results of Liver Absorbed Doses one-sample T test	34

LIST OF FIGURES

Figure 1.1. Generation of Bremsstrahlung	3
Figure 2.1. Basic principles and components of gama camera	12
Figure 2.2. SPECT/CT	13
Figure 2.3. Schematic representation of mutual annihilation reaction between a positron (β^+) and an ordinary electron	14
Figure 2.4. PET/CT	15
Figure 3.1. ^{90}Y microsphere treatment algorithm	17
Figure 3.2. VOIs for image analysis. VOIs for tumor (red), $^{99\text{m}}\text{Tc}$ -MAA area (green)	19
Figure 4.1. Tumor doses of $^{99\text{m}}\text{Tc}$ -MAA SPET/CT and ^{90}Y PET/CT	27
Figure 4.2. The graph of diffence and mean values in the 4.5 table and their place in the confidence interval.	28
Figure 4.3. Parenchyma doses of $^{99\text{m}}\text{Tc}$ -MAA SPET/CT and ^{90}Y PET/CT	30
Figure 4.4. The graph of diffence and mean values in the 4.8 table and their place in the confidence interval.	31
Figure 4.5. Liver doses of $^{99\text{m}}\text{Tc}$ -MAA SPET/CT and ^{90}Y PET/CT	33
Figure 4.6. The graph of diffence and mean values in the 4.11 table and their place in the confidence interval.	34

LIST OF SYMBOLS AND ABBREVIATIONS

SIRT = Selective Internal Radiation Therapy
 ^{99m}Tc -MAA = Technetium Macroaggregated Albumin
BSA = Body Surface Area
PM = Partition Model
LSF = Lung Shunt Fraction
REILD = Radioembolization-induced liver disease
RILD = Radiation induced liver disease
ROI = Region of Interest
VOI = Volume of Interest
SPECT = Single Photon Emission Computed Tomography
PET = Pozitron Emission Tomography
 ^{90}Y = Yittrium 90
HCC = Hepatocellular Carcinoma
GBq = Gigabecquerel
MIRD = Medical Internal Radiation Dose
mCi = Millicuries
FU = Fractional Uptake
TLR = Tumor liver ratio
BED = Biological effective dose
PR = Partial Response
CR = Complete Response
 γ ray = Gamma Ray
PM = Photomultiplier
NaI(Tl) = Sodium Iodide doped with Thalium
ADC = Analog to Digital Converter
 TiO_2 = Titanium Dioxide
keV = kilo electron volt
FOV = Field of view
TARE = Transarterial radioembolization

ABSTRACT

Ergiyen Buldu, G. (2019). Dosimetric Calculations in ^{90}Y Microsphere Treatment. Yeditepe University, Institute of Health Science, Department of Medical Physics, MSc thesis, İstanbul.

The aim of this study is to compare the mean absorbed doses of tumor, irradiated healthy parenchyma and whole liver obtained by $^{99\text{m}}\text{Tc}$ -MAA SPECT / CT and ^{90}Y PET / CT images before and after treatment in patients receiving ^{90}Y microsphere treatment. Patients with lung shunt fractions > 0.2 are excluded from the treatment. In total of 14 patients (8 females, 6 males, age: 35-76 years, totally 18 tumors) who underwent ^{90}Y microsphere treatment at Yeditepe University Hospital between May 2018 and February 2019 participated in the study. SPECT images are obtained by injecting an average of 185 MBq $^{99\text{m}}\text{Tc}$ -MAA during angiography. The required administered activities for SPECT images were calculated based on VOIs (Volume of Interests) for tumor, irradiated healthy parenchyma and whole liver using the partition method. After ^{90}Y treatment, PET / CT scan is performed and the absorbed dose was calculated with reference to $^{99\text{m}}\text{Tc}$ -MAA SPECT / CT images, areas for tumor, irradiated healthy parenchyma and whole liver using the same method as $^{99\text{m}}\text{Tc}$ -MAA SPECT. As a results; The absorbed dose of tumor, irradiated healthy parenchyma and whole liver calculated from PET / CT and SPECT counts were compared using Bland Altman method and 87.5% of the values were found to be within the confidence interval. In this study, it can be said that activity planning based on $^{99\text{m}}\text{Tc}$ -MAA SPECT is related to ^{90}Y microsphere PET / CT dosimetry calculated based on $^{99\text{m}}\text{Tc}$ -MAA SPECT areas. The ^{90}Y microsphere PET / CT-based post-treatment dosimetry, based on the $^{99\text{m}}\text{Tc}$ -MAA SPECT areas, is an effective method for predicting treatment efficacy.

Key words: ^{90}Y Microsphere Treatment, Dosimetric Calculations, Liver Cancer, Yttrium-90, Dosimetry

ÖZET

Ergiyen Buldu, G. (2019). ⁹⁰Y Mikroküre Tedavisinde Dozimetrik Hesaplamalar . Yeditepe Üniversitesi Sağlık Bilimleri Enstitüsü, Sağlık Fiziği ABD., Master Tezi. İstanbul.

Bu çalışmada ⁹⁰Y mikroküre tedavisi almış hastalarda tedavi öncesi ^{99m}Tc-MAA SPECT / CT ve tedavi sonrası ⁹⁰Y PET / CT görüntülerinden, tümör, ışınlanmış sağlıklı parankim ve sağlıklı tüm karaciğer ortalama soğurulan dozlarının karşılaştırılması amaçlandı. Akciğer şant fraksiyonları >0,2 olan hastalar tedaviden çıkarıldı. Çalışmaya Mayıs 2018, Şubat 2019 tarihleri arasında Yeditepe Üniversitesi Hastanesi'nde, ⁹⁰Y mikroküre tedavisi uygulanan toplam 14 hasta (8 Kadın, 6 Erkek, Yaş: 35-76 yıl) katıldı. Hastalara anjiyografi sırasında ortalama 185 MBq ^{99m}Tc-MAA enjekte edilerek SPECT görüntüleri elde edildi. SPECT görüntüleri kullanılarak hastalara uygulanması gereken aktivite, partitasyon metodu kullanılarak tümör, ışınlanmış sağlıklı parankim ve sağlıklı tüm karaciğer için VOI(Volume of Interest) çizilerek hesaplandı. ⁹⁰Y tedavisi sonrası PET / CT çekilerek doz miktarı ^{99m}Tc-MAA SPECT / CT alanları referans alınarak, aynı yöntem kullanılarak tümör, ışınlanmış sağlıklı parankim ve sağlıklı tüm karaciğer için hesaplandı. PET/CT ve SPECT sayımlarından hesaplanan tümör, ışınlanmış sağlıklı parankim ve sağlıklı tüm karaciğer doz miktarı Bland Altmann yöntemi kullanılarak karşılaştırıldı ve %85,7 oranında değerlerin güven aralığında olduğu tespit edildi. Bu çalışmada ^{99m}Tc-MAA SPECT'ye dayanan aktivite planlamasının, ^{99m}Tc-MAA SPECT alanları referans alınarak hesaplanan ⁹⁰Y mikroküre PET / CT dozimetri ile yakından ilişkili olduğu söylenebilir. ^{99m}Tc-MAA SPECT alanları referans alınarak yapılan ⁹⁰Y mikroküre PET / CT'ye dayalı tedavi sonrası dozimetri, tedavinin etkinliğini tahmin etmek için etkili bir yöntemdir.

Anahtar Kelimeler: ⁹⁰Y Mikroküre Tedavisi, Dozimetrik Hesaplamalar, Karaciğer Kanseri, Yttrium-90, Dozimetri

1. INTRODUCTION AND PURPOSE

In the body, the largest organ is liver. There are 2 lobes of liver that are typically described. Those were described by functional anatomy and by morphologic anatomy. Its location is in the upper right quarter of the abdominal cavity under the right hemidiaphragm. The position of it is maintained by peritoneal reflections which is called ligamento attachments have the protection of the rib cage (1).

Dual blood from the hepatic artery and portal vein makes the liver unique. 20% (approximately) of this dual blood is supplied from the hepatic artery and 80% (approximately) from the portal vein. The theoretical basis of this treatment is based on the feeding of malignant cells in the liver mainly from the hepatic artery and healthy hepatocytes from the portal venous system (2).

The prevalence of liver cancer in men is at the fifth place and it's at seventh place in women. It is considered that there are new cases between 250,000 and 1,000,000 every year. The liver's most prevalent primary cancer is Hepatocellular carcinoma when we think of the all primary liver cancers accounting from 85% till 90%. It is most common for people who are their 70s and it is rarely seen in people who are younger than 40. Chronic alcohol consumption, hepatitis c, hepatitis b and fatty non-alcoholic liver disease are the major risk factors for HCC (3).

^{90}Y microsphere treatment or SIRT(selective internal radiation therapy using ^{90}Y or ^{166}Ho) is an effective treatment for inoperable liver cancer. Many studies report therapeutic efficacy of ^{90}Y microsphere treatment (38-40) with rates of various therapy response in hepatocellular carcinoma, (41,42) and metastasis from colorectal cancer (3) or neuroendocrine tumors (4). Since the tumor is mostly supplied with blood from the hepatic artery, the ^{90}Y microsphere can be selectively delivered to the target lesion by angiographic intervention. The radionuclide ^{90}Y with a half-life of approximately 64 hours, 2.7 days and the maximum decay energy of 2.28 MeV. Various dosimetric methods, such as compartmental, non-compartmental or voxel based dosimetry is used to calculate the required activity to be administered in the treatment.

The aim of this study is to compare the average absorbed doses of tumor, irradiated healthy parenchyma and healthy whole liver from the $^{99\text{m}}\text{Tc}$ -MAA SPECT and post-treatment ^{90}Y PET/CT images before ^{90}Y microsphere treatment.

2. LITERATURE REVIEW

2.1. Yttrium-90 Physical Properties

There is a two way of ^{90}Y producing. One is the neutron bombardment of stable ^{89}Y and another way is chemical separation from its parent isotope strontium 90 (22). The half-life of ^{90}Y radionuclide is approximately 64 hours, 2.7 days. The maximum decay energy of 2.28 MeV is a rare-earth metal that chemically belongs to the lanthanides (25).

^{90}Y is considered as a pure β^- particle emitter although it emits 1.76 MeV γ photons and β^+ with abundances of 0.0078% and 0.0032%, respectively. The β^- particles from ^{90}Y decay has a mean energy of 0.94 MeV, average range of 2.5 mm and a maximum range of 11 mm tissue penetration in soft tissues (26). With this energy and range, the β^- particles can produce the “crossfire” effect. 90% of the energy is absorbed in a 5.3 mm radius sphere. Although the ^{90}Y isotope is a β^- releasing isotope, it also decays through the internal double formation. The branching ratio of the internal double formation is approximately 32×10^{-6} . Gamma rays with 511 keV energy due to positron disappearance can be imaged with PET system.

Pair production creates opportunity for ^{90}Y to be used in clinic. One of the usage area of ^{90}Y is in clinical studies to treat the patients have primary tumors like hepatocellularcarcinoma, cholangiocarcinoma and metastatic tumors of liver like colorectal metastasis, neuroendocrine metastasis, breast metastasis. In clinic ^{90}Y is labelled with microspheres to treat the patients with liver cancer in the Nuclear medicine department. Positron emission tomography (PET) imaging has recently been used to evaluate the distribution after ^{90}Y microsphere treatment (22-23). PET/CT imaging is the most common way to determine microsphere distribution after ^{90}Y microsphere injection (20-24).

2.1.1. Bremsstrahlung Radiation

When a high-speed electron passes near the nucleus, it is deflected from the electron path due to the gravitational force of the nucleus, causing an acceleration. An accelerated charge also emits electromagnetic radiation, ie it emits a photon. This radiation is called the Bremsstrahlung radiation or the white radiation. It causes a continuous x-ray spectrum. The probability of Bremsstrahlung emission per atom is proportional to Z of the absorber and energy of the particle.

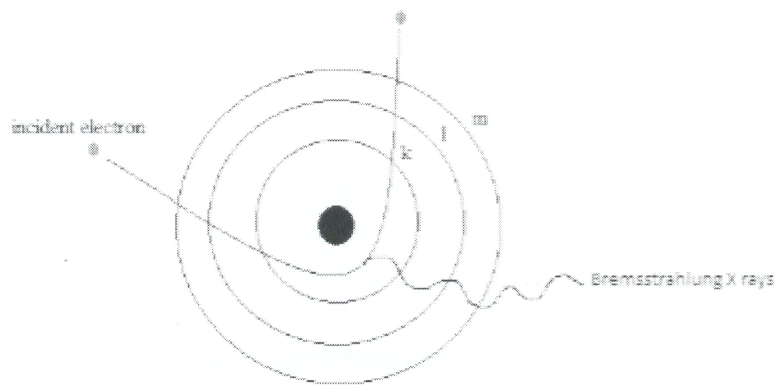


Figure 1.1. Generation of Bremsstrahlung

2.2. ^{90}Y Microspheres

Resin based microspheres are acrylic polymer microspheres in which the diameter is between 20 and 60 μm and ^{90}Y is bonded to the polymer carboxylic group after microspheres production. Glass microspheres are medium-sized glass microspheres of 20 to 30 μm , in which the ^{89}Y is embedded in the glass matrix and activated to ^{90}Y in a nuclear reactor.

2.3. ^{90}Y Glass Microspheres

Yttrium-89 (^{89}Y) is mixed with ultra-pure aluminum oxide and silicon dioxide and then melted in an oven at 1500° C to produce glass ^{90}Y microspheres (TheraSphere). The embedded glass is allowed to cool then crushed and passed through a flame thrower, thus the glass particles melt and “spheridize”. Spheres with a diameter of 20 to 30 microns pass through the sieves and transform neutron bombardment embedded ^{89}Y into ^{90}Y . The ^{90}Y is embedded in a glass matrix and is less likely to leak from the microspheres (27). Since the neutron bombardment of aluminum and silicon is made in the glass matrix, there are also unwanted radioactive substances with a long half-life. (^{88}Y half-life 107 days, ^{154}Eu half-life 8 years). The Glass microspheres’s density is 3.6 g/dL, and this is about 3 times the blood density (1.05 g/dL). “The specific activity of the glass microsphere is approximately 2500 Bq per sphere at the time of calibration (28,29,31).

2.4. ^{90}Y Microspheres Treatment Procedure and Dosimetry

^{90}Y microsphere treatment takes the names of SIRT, TARE, radioembolization and ^{90}Y microsphere treatment in various sources.

2.4.1. Administration of ^{90}Y microsphere

The essential steps of ^{90}Y microsphere treatment applied in this study include;

- (1) Patient Selection
- (2) Tumor Mapping – Angiography with $^{99\text{m}}\text{Tc}$ -MAA SPECT/CT Imaging
- (3) ^{90}Y Microsphere Treatment
- (4) ^{90}Y PET/CT Imaging
- (5) Post Treatment Care

The main goal of treatment is to maintain the liver tissue at the maximum level while giving the maximum dose to the liver tumor and minimum level to healthy liver. To ensure safe and accurate treatment, vascular mapping allows accurate calculation of target volumes. In addition, aortic angiography and hepatic arterial catheterization were performed to ensure safe and accurate delivery of ^{90}Y microspheres.

2.5. Patient Selection of ^{90}Y Microsphere Treatment

Only patients with no chance of surgery, life expectancy greater than 12 weeks, and lung shunt <0.2 were considered eligible candidates for the ^{90}Y microsphere treatment.

2.6. Before ^{90}Y Microsphere Treatment

$^{99\text{m}}\text{Tc}$ -MAA injection and angiography were performed for treatment planning. Before treatment, the lung shunt fraction must be calculated. Patients with lung shunt fractions (LSF) greater than 0.2 were excluded from the ^{90}Y microsphere treatment. Activity planning of the ^{90}Y microsphere treatment was based on the $^{99\text{m}}\text{Tc}$ -MAA SPECT / CT images. ^{90}Y Microsphere treatment was performed approximately 1-2 weeks after $^{99\text{m}}\text{Tc}$ -MAA SPECT study.

Approximately 185 MBq ^{99m}Tc -MAA injection and angiography planning was performed by the interventional radiologist (according to published guidelines) (35). Mesenteric angiography should be performed on patients who are candidates for patient ^{90}Y microsphere treatment. This is primarily done to identify anatomical variants, document visceral anatomy, and isolate hepatic circulation by occluding extrahepatic circulation. This information can usually be obtained from cross-sectional imaging. The celiac body is selectively catheterized to evaluate hepatic arterial supply of tumors (35).

The ^{90}Y microsphere treatment should be performed in such a same way with ^{99m}Tc -MAA angiography that the tumor will receive the highest dose. However, normal liver parenchyma will also be irradiated after this treatment, the dose of treatment should be planned according to tumor burden. If low tumor burden is present, more selective applications may be possible, for example at the segmental artery level.

For hepatic toxicity, there were four studies with data suitable for meta-analysis, and three studies with data total response dosimetry of HCC. In these literature, it is said that administrating greater than 205 Gy for glass microspheres increases dose response Mir and et al. also implied that the literature consistently supports that resin and glass microspheres produce treatment response and hepatotoxicity at different doses, a finding that was seen in the meta-analysis. In the dosimetry literature, the Y-90 PET / CT dosimetry defines doses less than 70 Gy as a safe dose for the non-tumor liver. These results are also consistent with the meta-analysis findings. Meta-analysis also supported the literature in which PET / CT metabolic profiling predicts tumor radiosensitivity.

Vascular mapping with adequate arterial phase CT scan is important to accurately calculate target volumes and ultimately plan the correct treatment. Hepatic artery anatomy includes variables and anomalies in the blood flow from the liver to the intestines and liver. The possibility of ^{90}Y microspheres refluxing in the gastric or gastroduodenal circulation can cause very serious clinical consequences, including gastrointestinal bleeding, severe ulceration or pancreatitis.

Therefore, all patients should undergo aortic angiography to evaluate arterial variants. This should be essential to ensure safe and accurate delivery of the ^{90}Y microspheres. (10)

HCC is characterized by arteriovenous shunting bypassing the capillary bed. In the case of arteriovenous shunt, both lungs are uniformly perfused through the vena cava, heart and lung arteries (45). This shunt in the lungs will increase the likelihood of radiation pneumonitis after the injection of ^{90}Y microspheres. For this reason, it is very important to determine and measure the lung shunt before treatment planning. This is accomplished by injecting $^{99\text{m}}\text{Tc-MAA}$ during angiography; 75-150 MBq $^{99\text{m}}\text{Tc-MAA}$ is administered via the hepatic catheter to the appropriate hepatic artery (or any branch of the hepatic artery when super- or hyper-selective therapy is planned). Since the size of the $^{99\text{m}}\text{Tc-MAA}$ particles closely mimics those of the ^{90}Y microspheres, the liver-lung shunt is evaluated by planar and / or tomographic (SPECT) images.

If there is a multifocal HCC, liver-lung shunt should be evaluated at the level of lobar before each treatment. The lung shunt fraction (LSF) is calculated by following equation 1:

$$\text{Lung Shunt Fraction} = \frac{\text{lung counts}}{\text{lung} + \text{liver counts}} \quad (1)$$

Without the attenuation correction, the LSF estimate gives a closer estimate than the weakening correction evaluations. Scatter correction may be important for the right lung, which is strongly affected by liver photon emission. Labeling should be done just before the application and scintigraphy should be performed immediately after angiography. In the $^{99\text{m}}\text{Tc-MAA}$ image, the visibility of the thyroid, stomach, body circumference and bladder allow measurement of the degree of free pertechnetate in the circulation. ^{90}Y microspheres can be applied when the possibility of extrahepatic shunting is evaluated in the interventional radiology department and the patient accepts treatment. Individually calculated activities are used according to the patient. If the main hepatic artery is injected, radiation is emitted to the two lobes of the liver. If there are only lesions in one lobe, the catheter is preserved contralateral so that it can be inserted selectively into the left or right lobar artery, which allows feeding of the affected lobe. In some cases, hyperselective (ie, single-segment) treatments can be performed. Soft infusion should be performed using the device specially designed to prevent backflow. There are differences depending on product characteristics in the application of two types of ^{90}Y microspheres. The specific activity is much lower, as

resin-based microspheres (SIR Spheres) contain less amount of ^{90}Y than glass microspheres (TheraSphere). Therefore, for the same amount of injected activities, these two types of ^{90}Y microspheres produce significantly different embolic loads. The mechanism of action of these two ^{90}Y microspheres is different. A thorough understanding of these differences will help to decide which device can best be applied to which patient.

Depending on the patient's life expectancy, tumor response and condition, treatment can be broken down or repeated. The risk of invasive and bulky intra-arterial administration should be considered. It should be noted that hypervascular lesions preserve more spheres. This may result in a higher tumor than the normal liver ratio.

For the normal hepatic parenchyma, the actual absorbed dose should be accurately estimated and the activity adjusted accordingly. In subsequent treatments, if the tumor hypervascularity is reduced, the amount of normal parenchymal tissue can be increased if the microspheres are less absorbed by the tumor or the same amount of activity is administered. It is recommended to repeat $^{99\text{m}}\text{Tc}$ -MAA scans if the treatment is repeated (4).

2.7. Dosimetric Calculations

2.7.1. Empirical Methods

Empirical methods have been tested for resin microspheres and are based on rough estimation of tumor rate (T) in the liver. The rate of tumor in the liver:

$$T = \frac{\text{tumour volume}}{\text{tumour volume} + \text{healthy liver volume}} \quad (2)$$

In the first empirical method defined for SIR-Sphere®, the recommended activity to be given to the patient according to the tumor rate is indicated as in Table 2.1:

Table 2.1. Recommended activity for treatment according to tumor burden

Tumor Burden (T)	Recommended Activity	
	GBq	mCi
T<0.25	2.0	54
0.25<T<0.5	2.5	68
T>0.5	3.0	81

Another empirical method defined for SIR-Sphere® is based on the size of the patient's body surface area (BSA). Recommended activity to be given to the patient for whole liver (bilobar) treatment:

$$A(GBq) = (BSA - 0.2) + \frac{\text{tumourvolume}}{\text{totallivervolume}} \quad (3)$$

is calculated by this equation. Here BSA is in m² and is calculated by the following relation:

$$BSA[m^2] = 0,20247 \times (\text{height}[m])^{0.725} \times (\text{weight}[kg])^{0.425} \quad (4)$$

Activity in the lobar or super-selective applications:

$$A(GBq) = \left[(BSA - 0.2) + \frac{\text{tumourvolume}}{\text{volumeoflobe}} \right] \times \left[\frac{\text{volumeoflobe}}{\text{totallivervolume}} \right] \quad (5)$$

is calculated with this equation.

Empirical methods have been used in studies where objective response and low toxicity have been reported. Nevertheless, due to the basis of the method, patients will be at risk of being exposed to unnecessary toxic dose or inadequate treatment activity. It should be kept in mind that tumor involvement rate is not taken into consideration in empirical methods. For this reason, dosimetric methods are generally recommended.

2.7.2. Dosimetric Methods

Dosimetric method can generally be examined under three headings:

1. Non-compartmental MIRD macro dosimetry
2. Compartmental MIRD Macro dosimetry
3. Dosimetry at the voxel level

2.7.2.1. Non-compartmental MIRD macro dosimetry

The non-compartmental MIRD macro dosimetry method was proposed by Salem et al. for glass ⁹⁰Y microspheres. The total dose amount to be exposed to the liver by the assumption that the activity given to the whole liver according to the method is uniformly distributed:

$$D_{liver} = \frac{A_0[GBq]}{m_{liver}[kg]} \times 49.37 \left[\frac{Gy.kg}{GBq} \right] \quad (6)$$

A_0 is injected activity, m_{liver} is the mass of the liver, the 49.37 constant is the dose factor per unit of activity in which ^{90}Y microspheres remain in capillary in the liver and only in the case of physical decay. For practical use, this factor is taken as 50.0 Gy·kg/GBq according to the EANM guideline (4).

According to the patient's medical condition, the recommended treatment dose is between 80 and 150 Gy. This dose is not the tumor dose, but the average dose of the whole liver. In the case of lobar or selective treatment, the liver mass in Equation 6 is replaced by the liver mass to which the treatment is administered. In this case, the dose to be calculated will be the average dose of the respective volume.

Pulmonary shunt fraction is determined from planar $^{99\text{m}}\text{Tc-MAA}$ scintigraphy. For this purpose, anterior and posterior planar images of the liver and lung areas of interest (ROI) are drawn and the geometric mean of the anterior and posterior counts are obtained. Pulmonary shunt fraction then calculated from these averages (lung shunt fraction, LSF):

$$\text{Lung Shunt Fraction} = \frac{\text{lung counts}}{\text{lung} + \text{liver counts}} \quad (7)$$

In this case Equation 6 for liver :

$$D_{liver} [\text{Gy}] = \frac{A_0 \times 50}{m_{liver} [\text{kg}]} \times (1 - \text{LSF}) \quad (8)$$

For lung :

$$D_{lung} [\text{Gy}] = \frac{A_0 \times 50}{m_{lung} [\text{kg}]} \times (1 - \text{LSF}) \quad (9)$$

Lung mass is used as 1 kg for lung dose calculations. In the treatment of glass ^{90}Y microspheres, the lung dose in a treatment should not exceed 30 Gy and this is an empirically determined limit value. In multiple irradiations this limit is applied as 50 Gy. For resin spheres, treatment activity is reduced according to LSF ratio.

The tumor dose is not known in the non-compartmental MIRD macro dosimetry method. One method to be used when calculating the tumor dose is the compartmental MIRD macro dosimetry.

2.7.2.2. Compartmental MIRD Macro dosimetry

In order to calculate the tumor dose, the distribution of activity in the liver should be divided into compartments such as tumor and healthy parenchyma. Tumor dose can be calculated by using the activity involvement ratios and the masses of compartments in these compartments:

$$D_{tumour} \cong \frac{50 \times A}{\frac{1}{TLR} \cdot (m_{parenchyma} + TLR \cdot m_{tumour})} \cdot (1 - LSF) \quad (10)$$

TLR is the tumor-parenchymal activity uptake rate. TLR can be determined from ^{99m}Tc -MAA SPECT study using 3-dimensional volumes of interests (VOIs).

The Compartmental MIRD macro dosimetry method can be used for resin and glass microspheres. Besides the tumor dose, it is possible to calculate the healthy parenchyma injected with the activity and the healthy whole liver dose. Treatment planning can be optimized by taking these parameters into account in addition to the tumor dose.

The compartmental MIRD macro dosimetry method assumes that the dose distribution for tumor and parenchymal compartments are homogeneous. The heterogeneous distribution within the tumor or the tumors in different locations cannot be evaluated within one compartment and the differences in involvement between them are not taken into consideration. In order to achieve this, dosimetry should be performed at the voxel level.

2.7.2.3. Dosimetry at the voxel level

Internal dosimetry at the voxel level allows the determination of heterogeneous dose distributions in the organs. Unlike the MIRD method, the distribution of activity (and therefore dose) within the organ is not considered to be homogeneous. There are 3 basic methods for dosimetry at the voxel level:

1. Local energy accumulation method
2. Dose-Point Kernel (DPK) convolution method
3. Monte Carlo (MC) method

The local energy accumulation method is the simplest and the accuracy is limited. According to this method, the alpha and beta particles give their energy into the voxel where they are released from the radioactive material core. Dose absorption in neighboring voxels is ignored.

In the Dose-Point Kernel (DPK) convolution method, the point dose distributions of a point source in an environment are determined by Monte Carlo method. These distributions are often referred to as the voxel S factor and are usually calculated for water. With the convolution of the additives from all voxels, the dose distribution in the volume of interest is determined. The weakness of this method is that only a single environment is calculated and cannot take into account tissue heterogeneity. (37)

Monte Carlo method is the most accurate but the most time-consuming vocal level dosimetry method. In the MC method, radiation distribution is performed using the distribution of activity in quantitative SPECT images and the physical density map of the body in the paired CT images (which can be calculated from Hounsfield Unit values). Depending on the isotope used, all the SPECT voxels release particles (such as beta, Auger electron, alpha) and photons (gamma and x-rays), the possibility of interaction with the CT image in the determined environment (photoelectric event, Compton scattering, Bremsstrahlung photon production). The amount of energy they transfer to the environment voxels are calculated as stochastic. This energy gives the absorbed dose in each voxel. This method is time consuming because it is necessary to calculate the accuracy of calculation statistics by transporting hundreds of millions or more of particles and photons one by one.

2.8. Reference Values

The tolerance limits for ^{90}Y microsphere treatment are the dose requirement (> 120 Gy) absorbed for lung treatment (<20 Gy), target normal liver (<70 Gy), and also for tumor treatment (33). In some cases where the normal intra-target liver volume is quite small, the tolerance limit (<30 Gy) of the non-target normal liver may be taken. (34)

Table 2.2. Tolerance limits for ^{90}Y microsphere treatment

Lung	<20 Gy
In-target normal liver	<70 Gy
Absorbed dose requirement for tumor treatment	>120 Gy
Out-target normal liver	<30 Gy

For tumor response there are few threshold values and liver toxicity in microsphere treatment. EBRT Emami et al. (14) showed that in the hypothetical case of a uniform irradiation in the liver, the 5% risk threshold for radiation-induced liver disease (RILD) is at an average 30 Gy liver dose; 50% of the patients are at 43 Gy. The whole liver tissue uniform irradiation is not the same as microspheric radioembolization.

2.9. Radionuclide Imaging

The purpose of radionuclide imaging is to display the distribution of the radioactively labeled substance in the body.

2.9.1. Gama Camera

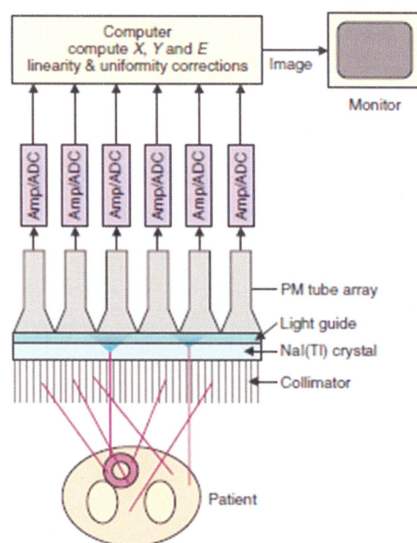


Figure 2.1. Basic principles and components of gama camera (19)

According to this diagram (Figure 2.1), the gamma photons emitted from the organ are directed by the collimator and reduced to the detector element NaI crystal. By stopping gamma photons falling on the crystal (photoelectric effect or Compton scattering), scintillation photons are proportional to their energy. The positions of the scintillation events occurring are determined by the photomultiplier tube and the position logic circuit located behind the crystal. The scintillation photons are struck in

the photocathode at the inlet of the PMTs, causing electron breakage therefrom. The released electrons are accelerated by the effect of high voltage between the dynods in the PMT and gradually increase in number. In this way, the electrons are transported to the anode at the PMT outlet. Thus, gamma photons are converted to scintillation photons in NaI crystal and converted into electrical signals through PMT. These signals are amplified and shaped in various electronic units and then converted into images.

Basic Parts of Gamma Camera are collimators, scintillation crystal, photomultiplier tube, puls height analyzers, computer, amplifier, preamplifier.

2.9.2. SPECT/CT

The most important and essential part of SPECT systems is the gamma camera detector. A single gamma camera head is mounted on a rotating portal, which provides the data required for tomographic images. The gamma camera rotates at equal angular intervals around the patient to obtain a two-dimensional (2-D) projection image. These images provide the 1B projection data needed to recreate the sectional images. Typically, clinical SPECT images are reconstructed in a 64 x 64 or 128 x 128 pixel matrix. Cross-sectional images are generated for all axial positions (slices) covered by the field of view (FOV) of the gamma camera, leading to a stack of adjacent 2D images that make up the 3D image volume.

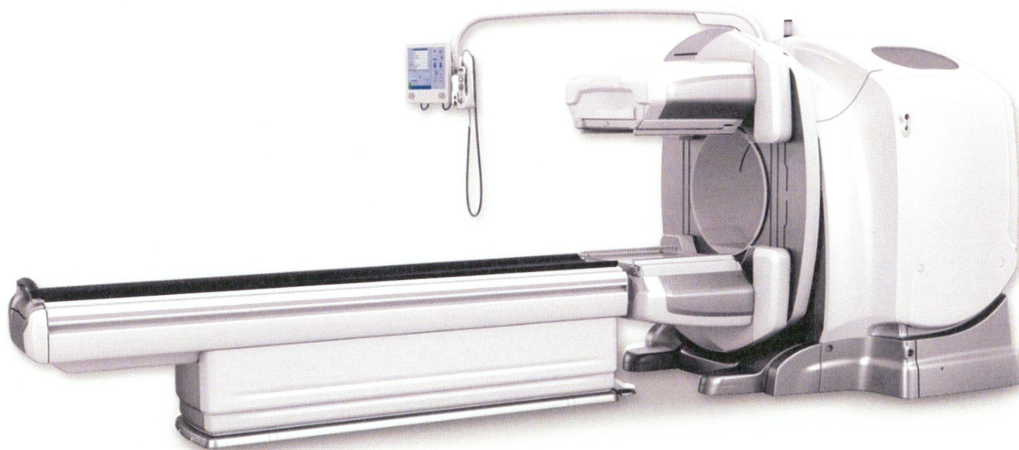


Figure 2.2. SPECT/CT (44)

2.9.3. PET/CT

Positron Emission Tomography (PET) is a modern nuclear medicine imaging technique based on the principle of the detection of a pair of 511 keV-energy annihilation photons. PET offers numerous advantages to clinicians over other imaging systems. In this technique, molecular imaging of a biological function in the body is performed. Therefore, the sensitivity of PET images is higher than other imaging techniques. Radiopharmaceuticals used for imaging purposes are expected to be kept at the maximum level in the target organ and at a minimum level in the other organs. Therefore, scintigraphic separation becomes difficult in other regions except the body areas where the radiopharmaceutical is heavily involved. However, anatomical separation of the radiopharmaceutical is often not possible. Computed tomography (CT) images are used to interpret PET images. For this purpose, PET and CT images of the same section are overlapped (fusion) to obtain the source of the correct information in PET images. In positron emission tomography imaging, radiopharmaceuticals that emit positron (β^+) emitting beta particle (+) charged to the body are given. For example, ^{18}F and ^{68}Ga are widely used PET radiopharmaceuticals that release β^+ when disintegrated (44).

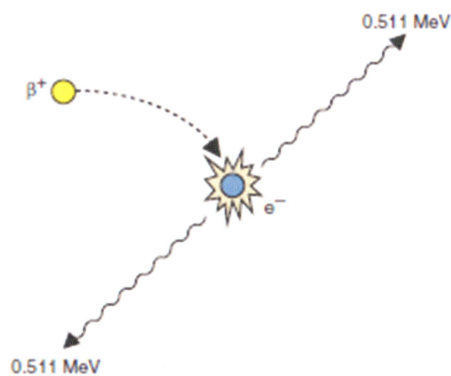


Figure 2.3. Schematic representation of mutual annihilation reaction between a positron (β^+) and an ordinary electron. A pair of 0.511-MeV annihilation photons are emitted “back-to-back” at 180 degrees to each other. (44)



Figure 2.4. PET/CT

3. MATERIALS AND METHODS

3.1. Patients

In total 14 patients (8 Female, 6 Male, Age: 35-76 year) who had ^{90}Y microsphere treatment at the Yeditepe Hospital involved in this study between May 2018 and February 2019. The detailed information related to patients are given in Table 3.1. Tumor and liver volumes for each patient were measured by using CT images.

Table 3.1. Specific characteristics of patients, HCC : Hepatocellular carcinoma

Patient number	Age	Type of Cancer	Tumor Volume (cm ³)	Liver Volume (cm ³)
1	52	HCC	318.4	1780.0
2	64	HCC	27.5	2726.0
3	46	HCC	98.8	1354.0
4	66	Colon CA	186.2	1620.0
5	66	Colon CA	338.1	1379.0
6	76	Colon CA	25.5	1668.0
7	70	Colon CA	360.3	2390.0
8	67	Colon CA	39.2	1440.0
9	46	cholangiocarcinoma	414.7	1348.9
10	47	Breast Malignant Neoplasm	281.8	1530.0
11	57	Neuroendocrine CA	348.4	2100.0
12	35	Meduller Thyroid CA	50.7	1331.0
13	49	Malignant Melenoma	47.9	2040.0
14	51	Rectum CA	94.1	1500.0

The mean age of the patients is 56.6 ± 11.6 , the mean tumor volume is 188.0 ± 142.6 cm³ and the mean liver volume is 1729.1 ± 416.2 cm³.

3.2. ^{90}Y Microsphere Treatment Algorithm

The ^{90}Y microsphere treatment algorithm is given in Figure 3.1.

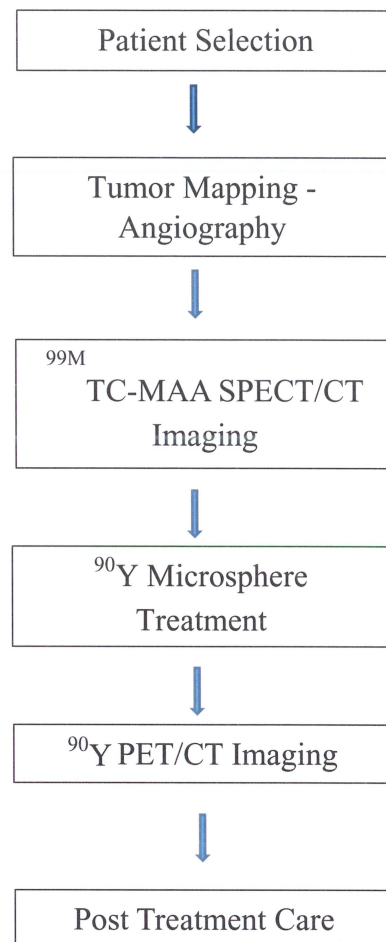


Figure 3.1. ^{90}Y microsphere treatment algorithm

3.3. Patient Selection for ^{90}Y microsphere treatment

Selection criteria of the patients:

1. Limited extra-hepatic disease
2. Life expectancy of at least 3 months
3. Enough hepatic reserve
4. Sufficient vascularisation of the tumors
5. Bilirubin level

3.4. Tumor mapping - Angiography

Planning angiography should be performed 1-2 weeks before treatment. Catheterization of the hepatic artery via the femoral artery is performed in the angiography laboratory before treatment. During the injection of the main hepatic artery, radiation is distributed to liver lobes included tumor. If the lesion is confined to a single lobe, the catheter is selectively placed in the left or right hepatic artery of the respective lobe. Hyperselective therapies can be applied in selected patients if there is a single segment limited disease.

The patient is evaluated for arterial anatomy, blood supply to extrahepatic organs and, if necessary, embolized vascular branches to provide redistribution or prevent possible leakages. Hepatic arterial mapping, embolization of non-target vessels, ^{99m}Tc -MAA should be applied to simulate microsphere deposition. Investigation of undesirable clinical toxicities such as gastric ulceration, pancreatitis, skin irritation and pulmonary edema are necessary to reduce the risk of radiation pneumonia. Celiac angiography evaluates the origin and parasitization of accessory or replicated left hepatic artery, medial and lateral segmental branches of the left hepatic artery from separate origins. Angiography can be used as a noninvasive test in treatment planning with high-speed multislice CT (Cone beam CT-angiography).

3.5. ^{99m}Tc -MAA SPECT/CT Imaging

For all patients with the injection of average was 185 MBq of ^{99m}Tc -MAA in one or more branch of hepatic artery which the segment of the tumor, and scintigraphy was performed for lung shunt fraction, tumor distribution and extravascular leakage during the angiography procedure. It is assumed that the size of the ^{99m}Tc -MAA particles is nearly similar to the size of the ^{90}Y microspheres. The lung shunt is evaluated with SPECT / CT images.

After administration of ^{99m}Tc -MAA anterior and posterior whole body planar images and SPECT were acquired on Philips Forte Gama Camera. The acquisition duration was 8 min for whole-body and 22 min for SPECT (30 sec/projection). In addition, CT scan was performed for anatomical correlation with GE Discovery IQ PET/CT system. The images were reconstructed with Maximum-Likelihood Expectation-Maximization (ML-EM) iterative reconstruction algorithm with 20

iterations. A post- reconstruction Butterworth filter with a cut-off frequency 0.50 and order 5 were applied on images.

3.6. Dose Calculation and Planing Volume Determination

Partition model method was used for activity planning. 3 partitions were defined in the liver: tumor, in-target normal liver defined as the non-tumorous liver supplied by the target artery of ^{90}Y microsphere treatment, and out-target normal liver defined as the non-tumorous liver supplied by nontarget arteries of ^{90}Y microsphere treatment. On $^{99\text{m}}\text{Tc}$ -MAA SPECT/ CT images, VOIs of these 3 partitions were drawn manually (can be seen in Figure 3.2.).

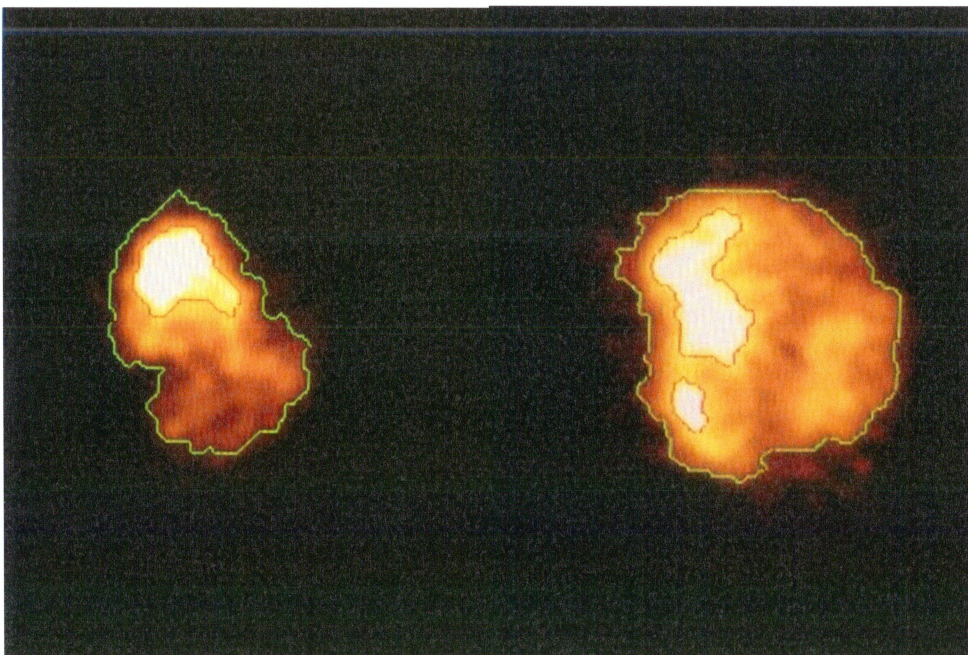


Figure 3.2. VOIs for image analysis. VOIs for tumor (red), $^{99\text{m}}\text{Tc}$ -MAA area (green),

Mean uptake in counts per unit volume in the tumor (C_{tm}), in-target normal liver (C_{in}), and out target normal liver (C_{out}) including corresponding volumes (V_{tm} , V_{in} , and V_{out}) were measured based on drawn VOIs.

These information were used to calculate the absorbed dose of each partition by using the Eq. (11) :

$$D_{liver} [Gy] = \frac{\text{injected activity} [GBq] \times 50 \times \left(\frac{C_{im} V_{im}}{C_{im} V_{im} + C_{in} V_{in} + C_{out} V_{out}} \right) \times (1 - LSF) \times (1 - Residual)}{\frac{m_{liver}}{1000} \left[\frac{cm^3}{g} \right] \times 1,03} \quad (11)$$

(1-Residual) = assuming 1% of the given dose remains in the catheter

1,03 = Liver tissue density (for using kg to cc)

Dose for the in-target normal or out-target normal liver was also calculated using the same method.

3.7. ⁹⁰Y PET/CT Imaging

Calculated treatment activities were injected to the patients. Immediately after completion of ⁹⁰Y microsphere treatment with the injection of ⁹⁰Y, PET/CT images were obtained by GE Discovery IQ PET/CT scanner. CT images were acquired first in a spiral mode (120 kVp, and 70 mAs). PET images were acquired for 15 minutes per bed in 3D mode. CT images were reconstructed using a conventional filtered back projection method, 50-cm field of view and 3.8-mm increment per slice. Q.Clear reconstruction algorithm was applied to PET images. ⁹⁰Y PET/CT counts of tumor, in-target normal liver, and out target normal liver were measured according toVOIs defined by ^{99m}Tc-MAA SPECT/CT images. By using the mean number of counts and volume information absorbed dose values were calculated for each patient.

Q.Clear is a Bayesian penalized likelihood (PL) reconstruction algorithm. This algorithm ensures that the algorithm reaches full convergence without the harmful effects of noise and providing superior image quality while keeping background image noise low. Q.Clear uses the Block Sequential Regularized Expectation Maximization (BSREM) algorithm to solve BSREM algorithm allows every single image voxel to achieve 100% convergence despite OSEM that did not seek for convergence and may achieve partial convergence, full convergence or over convergence in one single image.

3.8. Bland-Altman Analysis

Dose values calculated with both methods were compared using Bland-Altman statistical analysis.

The most important features of the Bland - Altman method are that the two methods reveal measurement differences and leave the interpretation of the level of acceptability of the differences to the opinion of the clinician. The analysis should start with the scatter plot plotted against the means of the differences between the results of the two methods. These graphs allow you to examine whether the differences show a systematic distribution around zero and the extent to which they are. The degree of correlation depends on the extent of distribution of the results in the sample. Although the two samples had poor agreement, they showed high correlation. The test of the significance of the correlation coefficient is the test of the hypothesis that there is no correlation between the two methods. It is unnecessary to test whether two methods designed to measure the same value are correlated. The agreement between the two methods can be examined using the mean (d) and standard deviation (s) of differences. When the method B is used, the measured value is calculated from the value obtained with A; d - as small as $1.96 s$ or as large as $d + 1.96 s$. In this method, " $d + 1.96 s$ " is called compliance limits. Generally, correlation and regression analysis are used to determine compliance level. Generally, medical laboratories use this analysis to determine the similarity between two different measurement methods. (36)

One sample T Test is one of the step of Bland Altman method. It can be defined as an approach that tries to determine statistically whether there is a significant difference between the means of the two groups of data. This test is generally applied to test the accuracy of this prediction when certain predictions are made on any subject. For instance; it is known that the average age of 5000 employees working in A facility is 37. Is the mean age of a randomly selected sample of 500 different from 37?

0.05 is the margin of error, and the resulting value p is expected to be greater than this. ($P > 0,05$)

Another step that regression analysis is used to put the relationship between one or more independent variables and a dependent variable as a mathematical equation.

4. RESULTS AND DISCUSSION

4.1. Treatment Activities

Considering the results of the Eqn 11 the required injected treatment activities for patient ^{90}Y microsphere treatment was calculated. The determined activities are given in Table 4.1.

Table 4.1. Required injected treatment activities for each patient based on $^{99\text{m}}\text{Tc}$ -MAA SPECT/CT images.

Patient No.	Treatment Activity (GBq)
1	1.78
2	1.21
3	0.58
4	2.22
5	2.05
6	0.92
7	3.79
8	1.50
9	3.15
10	2.06
11	2.03
12	1.96
13	2.53
14	1.29

The mean treatment activity of the patients is 1.9 ± 0.8 MBq.

4.2. Lung shunt fractions and lung doses

Lung shunt fraction and lung dose values are given in Table 4.2.

Table 4.2. Lung Shunt Fraction and Lung Dose value of patients

Patient No.	Lung Shunt Fraction(%)	Lung Dose(Gy)
1	11.0	9.7
2	6.0	3.6
3	5.0	1.4
4	10.0	11.0
5	5.0	5.1
6	5.0	2.3
7	9.0	16.9
8	4.0	3.0
9	4.0	6.2
10	3.0	3.1
11	8.0	8.1
12	5.0	4.9
13	2.0	2.5
14	2.0	1.3

The mean lung fraction of the patients is 5.6 ± 2.5 % and the mean lung dose is 5.6 ± 4.3 Gy. As seen in the table non of the patients exceed this tolerance limits.

4.3. Absorbed doses for each patient based on ^{99m}Tc-MAA SPET/CT images

Absorbed doses for each patient based on ^{99m}Tc-MAA SPET/CT images values are given in Table 4.3.

Table 4.3. Absorbed doses for each patient based on ^{99m}Tc-MAA SPET/CT images

Patient No.	Tumor Doses(Gy)	Parenchyma Doses(Gy)	Liver Doses(Gy)
1	163.1	54.7	13.7
2	562.5	252.6	14.3
3	134.1	77.9	9.7
4	176.4	63.5	39.0
5	140.0	63.0	33.4
6	756.0	208.5	13.5
7	179.0	78.8	42.4
8	187.6	92.2	42.9
9	214.2	67.7	41.7
10	120.4	67.2	40.5
11	134.7	55.1	20.5
12	317.6	68.8	55.3
13	243.3	93.9	52.7
14	166.4	67.7	30.0

Tumor, parenchyma and liver absorbed doses based on ^{99m}Tc-MAA SPET/CT images are given in the Table 4.4. The mean tumor dose of the patients on ^{99m}Tc-MAA SPET/CT images is 249.7 ± 178.1 , the mean parenchyma doses on ^{99m}Tc-MAA SPET/CT images is 93.7 ± 57.6 cm³ and the mean liver doses on ^{99m}Tc-MAA SPET/CT images is 32.1 ± 14.7 cm³.

4.4. Absorbed doses for each patient based on on ⁹⁰Y PET/CT images

Absorbed doses for each patient based on on ⁹⁰Y PET/CT images values are given in Table 4.4.

Table 4.4. Absorbed doses for each patient based on ⁹⁰Y PET/CT images

Patient No.	Tumor Doses(Gy)	Parenchyma Doses(Gy)	Liver Doses(Gy)
1	169.4	50.2	12.5
2	436.8	275.0	15.6
3	124.5	83.5	10.4
4	152.8	67.9	41.7
5	110.0	76.8	40.7
6	806.5	196.6	12.7
7	164.2	82.9	44.6
8	196.8	91.7	42.6
9	220.1	64.7	39.9
10	86.9	77.4	46.7
11	134.1	55.4	20.6
12	466.6	61.8	49.6
13	245.1	93.9	52.7
14	145.0	70.7	31.4

Tumor, parenchyma and liver absorbed doses based on ⁹⁰Y PET/CT images are given in the Table 4.3. The mean tumor dose of the patients on ⁹⁰Y PET/CT images is 247.1 ± 189.9 Gy, the mean parenchyma doses on ⁹⁰Y PET/CT images is 96.3 ± 60.1 Gy and the mean liver doses on ⁹⁰Y PET/CT images is 33.0 ± 14.8 Gy.

4.5. Tumor Absorbed Doses

We will compare the difference value between pre – post absorbed doses using the difference value in the t test. Tumor doses of pre-post dosimetry are given in the table 4.5.

Table 4.5. Tumor doses of pre-post dosimetry

Patient No.	Tumor doses (Gy) of ^{99m} Tc-MAA based dosimetry(A)	Tumor doses (Gy) of ⁹⁰ Y based dosimetry(B)	Difference Value (Gy)(A-B)	Mean Value (Gy) ((A+B)/2)(mmean)
1	163.10	169.40	-6.30	166.25
2	562.50	436.80	125.70	499.65
3	134.10	124.50	9.60	129.30
4	176.40	152.40	24.00	164.40
5	140.00	110.00	30.00	125.00
6	760.10	810.90	-50.80	785.50
7	179.00	164.20	14.80	171.60
8	187.60	196.80	-9.20	192.20
9	209.70	215.50	-5.80	212.60
10	155.90	112.50	43.40	134.20
11	134.70	134.10	0.60	134.40
12	317.90	467.10	-149.20	392.50
13	243.30	245.10	-1.80	244.20
14	166.40	145.00	21.40	155.70

A: Tumor doses (Gy) of ^{99m}Tc-MAA based dosimetry(A)

B: Tumor doses (Gy) of ⁹⁰Y based dosimetry(B)

Graph of tumor doses of ^{99m}Tc -MAA SPET/CT and ^{90}Y PET/CT is shown in the figure 4.1.

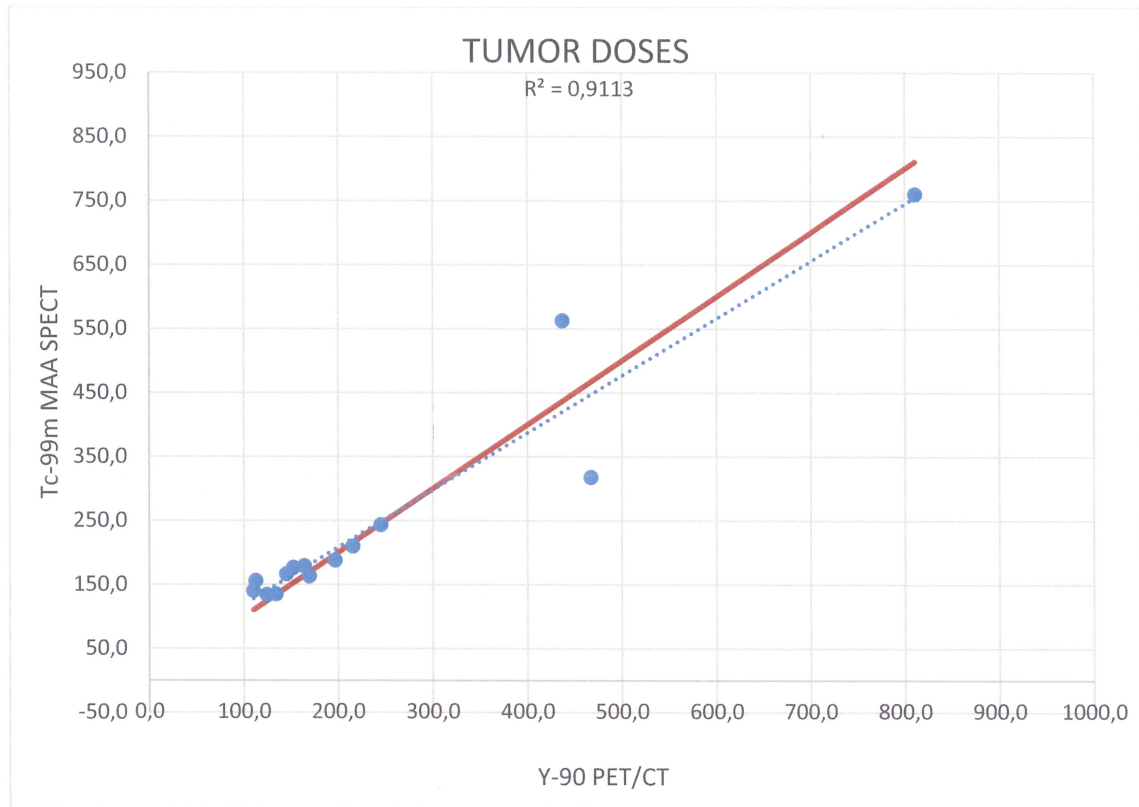


Figure 4.1. Tumor doses of ^{99m}Tc -MAA SPET/CT and ^{90}Y PET/CT (red line $x=y$)

Sample statistics results of absorbed tumor doses are given in table 4.6.

Table 4.6. Results of Tumor Absorbed Doses Sample Statistics

One-Sample Statistics				
	N	Mean	Std. Deviation	Std. Error
Difference	14	3.3143	58.68972	15.68549

N = number of sample

Mean = mean of differences

One-Sample Test results of absorbed tumor doses are given in table 4.7.

Table 4.7. Results of Tumor Absorbed Doses one-sample T test

One-Sample Test						
	Test Value = 0					
	t	Df	Sig. (2-tailed)	Mean Difference	95% Confidence Interval of the Difference	
					Lower	Upper
Difference	.211	13	.836	3.31429	-30.5721	37.2007

$p = \text{significance} > 0.05$

Since our value p is greater than 0.05, we can say that this study is meaningful.

The Bland Altman analysis graph of absorbed tumor doses is shown in the figure 4.2.

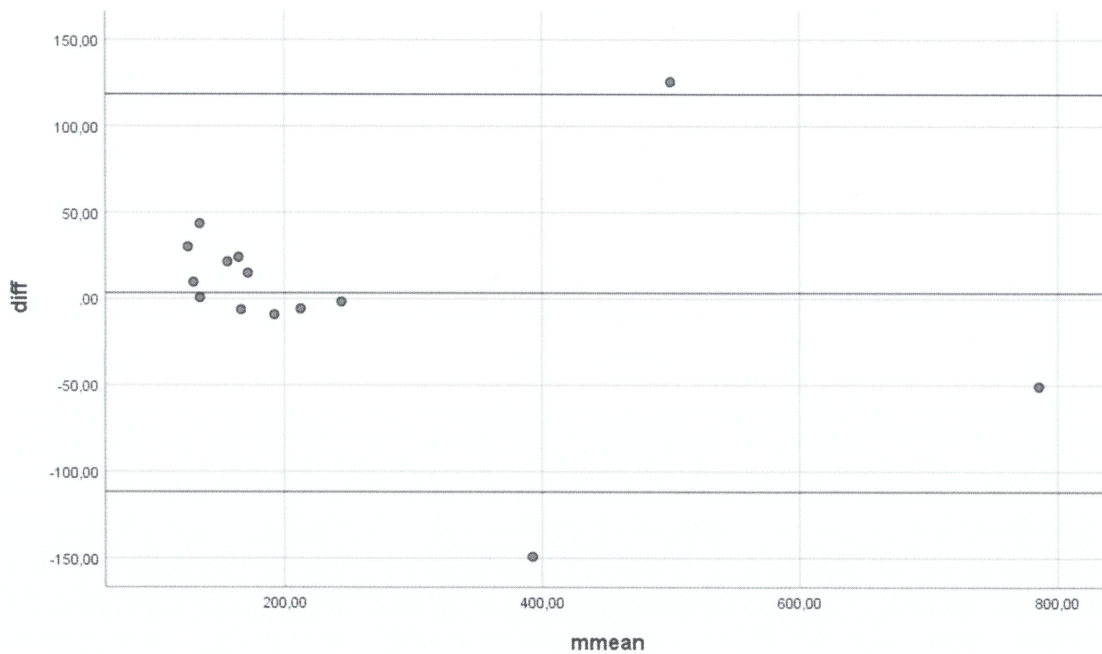


Figure 4.2. The graph of difference and mean values in the 4.5 table and their place in the confidence interval.

4.6. Parenchyma Absorbed Doses

We will compare the difference value between pre – post absorbed doses using the difference value in the t test. Parenchyma doses of pre-post dosimetry are given in the Table 4.8.

Table 4.8. Parenchyma doses of pre-post dosimetry

Patient No.	Parenchyma doses (Gy) of ^{99m} Tc-MAA based dosimetry(A)	Parenchyma doses (Gy) of ⁹⁰ Y based dosimetry(B)	Difference Value (Gy) (A-B)	Mean Value (Gy) ((A+B)/2)(mmean)
1	54.70	50.20	4.50	52.45
2	252.60	275.00	-22.40	263.80
3	77.90	83.50	-5.60	80.70
4	63.50	67.90	-4.40	65.70
5	63.00	76.80	-13.80	69.90
6	208.50	196.60	11.90	202.55
7	78.80	82.90	-4.10	80.85
8	92.20	91.70	0.50	91.95
9	67.70	64.70	3.00	66.20
10	67.20	77.40	-10.20	72.30
11	55.10	55.40	-0.30	55.25
12	68.80	61.80	7.00	65.30
13	93.90	93.90	0.00	93.90
14	67.70	70.70	-3.00	69.20

A: Tumor doses (Gy) of ^{99m}Tc-MAA based dosimetry(A)

B: Tumor doses (Gy) of ⁹⁰Y based dosimetry(B)

Graph of parenchyma doses of ^{99m}Tc -MAA SPET/CT and ^{90}Y PET/CT is shown in the Figure 4.3.

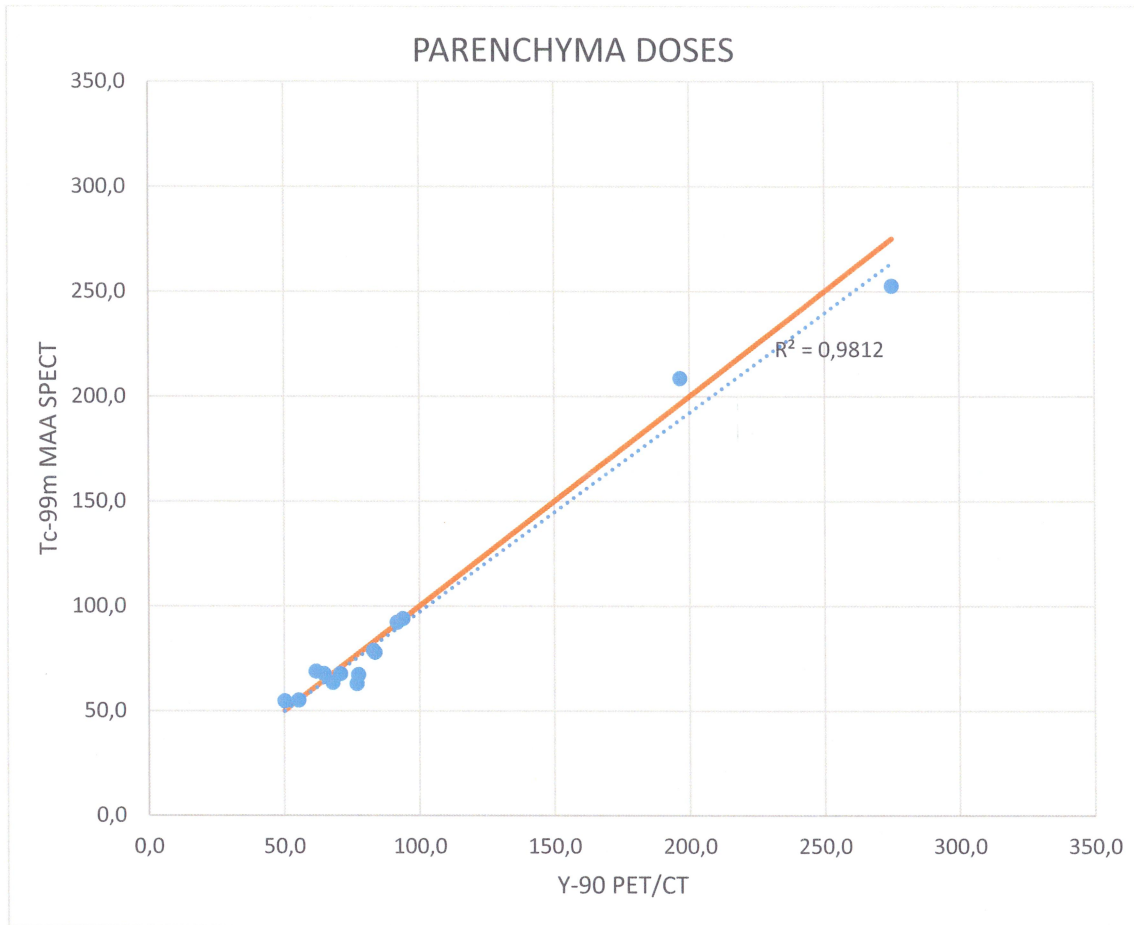


Figure 4.3. Parenchyma doses of ^{99m}Tc -MAA SPET/CT and ^{90}Y PET/CT (red line $x=y$)

Sample Statistics results of parenchyma absorbed doses are given in the Table 4.9.

Table 4.9. Results of Parenchyma Absorbed Doses Sample Statistics

One-Sample Statistics					
	N	Mean	Std. Deviation	Std. Error Mean	Error
Difference	14	-2.6357	8.75176	2.33901	

N = number of sample

Mean = mean of differences

One-sample T test results of parenchyma absorbed doses are given in the Table 4.10.

Table 4.10. Results of Parenchyma Absorbed Doses one-sample T test

One-Sample Test						
	Test Value = 0					
	T	df	Sig. (2-tailed)	Mean Difference	95% Confidence Interval of the Difference	
					Lower	Upper
Difference	-1.127	13	.280	-2.63571	-7.6888	2.4174

$p = \text{significance} > 0.05$

Since our value p is greater than 0.05, we can say that this study is meaningful.

The Bland Altman analysis graph of absorbed parenchyma doses is shown in the figure 4.4.

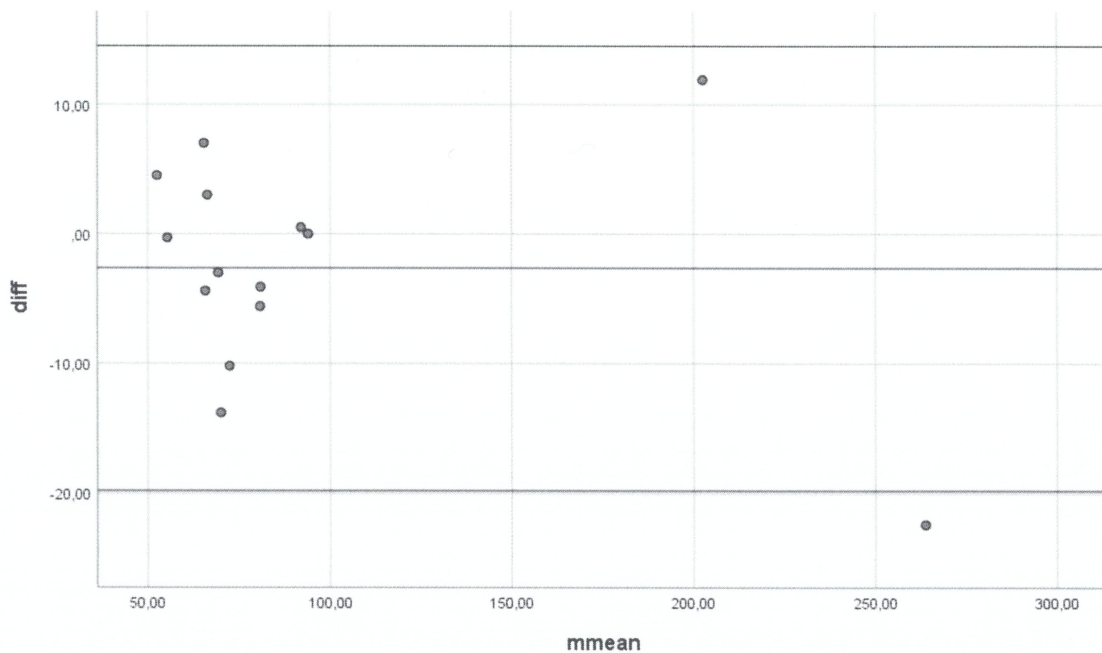


Figure 4.4. The graph of difference and mean values in the 4.8 table and their place in the confidence interval.

4.7. Liver Absorbed Doses

We will compare the difference value between pre – post absorbed doses using the difference value in the t test. Liver doses of pre-post dosimetry are given in the table 4.11.

Table 4.11. Liver doses of pre-post dosimetry

Patient No.	Liver doses (Gy) of ^{99m} Tc-MAA based dosimetry(A)	Liver doses (Gy) of ⁹⁰ Y based dosimetry(B)	Difference Value (Gy) (A-B)	Mean Value (Gy) ((A+B)/2)(mmean)
1	13.70	12.50	1.20	13.10
2	14.30	15.60	-1.30	14.95
3	9.70	10.40	-0.70	10.05
4	39.00	41.70	-2.70	40.35
5	33.40	40.70	-7.30	37.05
6	13.50	12.70	0.80	13.10
7	42.40	44.60	-2.20	43.50
8	42.90	42.60	0.30	42.75
9	41.70	39.90	1.80	40.80
10	40.50	46.70	-6.20	43.60
11	20.50	20.60	-.10	20.55
12	55.30	49.60	5.70	52.45
13	52.70	52.70	0.00	52.70
14	30.00	31.40	-1.40	30.70
15	13.70	12.50	1.20	13.10

A: Tumor doses (Gy) of ^{99m}Tc-MAA based dosimetry(A)

B: Tumor doses (Gy) of ⁹⁰Y based dosimetry(B)

Graph of liver doses of ^{99m}Tc -MAA SPET/CT and ^{90}Y PET/CT is shown in the Figure 4.5.

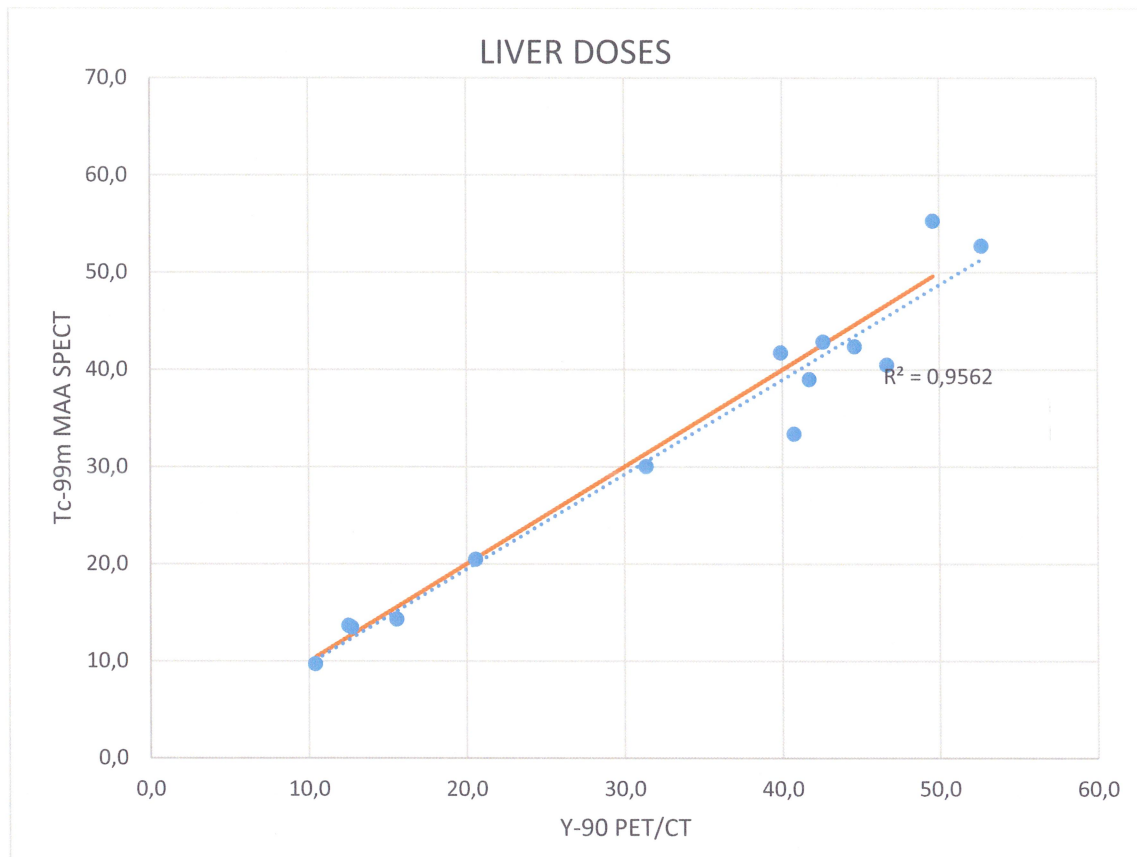


Figure 4.5. Liver doses of ^{99m}Tc -MAA SPET/CT and ^{90}Y PET/CT (red line $x=y$)

Sample Statistics results of liver absorbed doses are given in the table 4.12.

Table 4.12. Results of Liver Absorbed Doses Sample Statistics

One-Sample Statistics				
	N	Mean	Std. Deviation	Std. Error Mean
Difference	14	-.8643	3.22791	.86269

N = number of sample

Mean = mean of differences

One-sample T test results of liver absorbed doses are given in the table 4.13.

Table 4.13. Results of Liver Absorbed Doses one-sample T test

One-Sample Test						
	Test Value = 0					
	T	df	Sig. (2-tailed)	Mean Difference	95% Confidence Interval of the Difference	
Difference	-1.002	13	.335	-.86429	Lower -2.7280	Upper .9995

p=significance > 0.05

Since our value p is greater than 0.05, we can say that this study is meaningful.

The Bland Altman analysis graph of absorbed liver doses is shown in the figure 4.6.

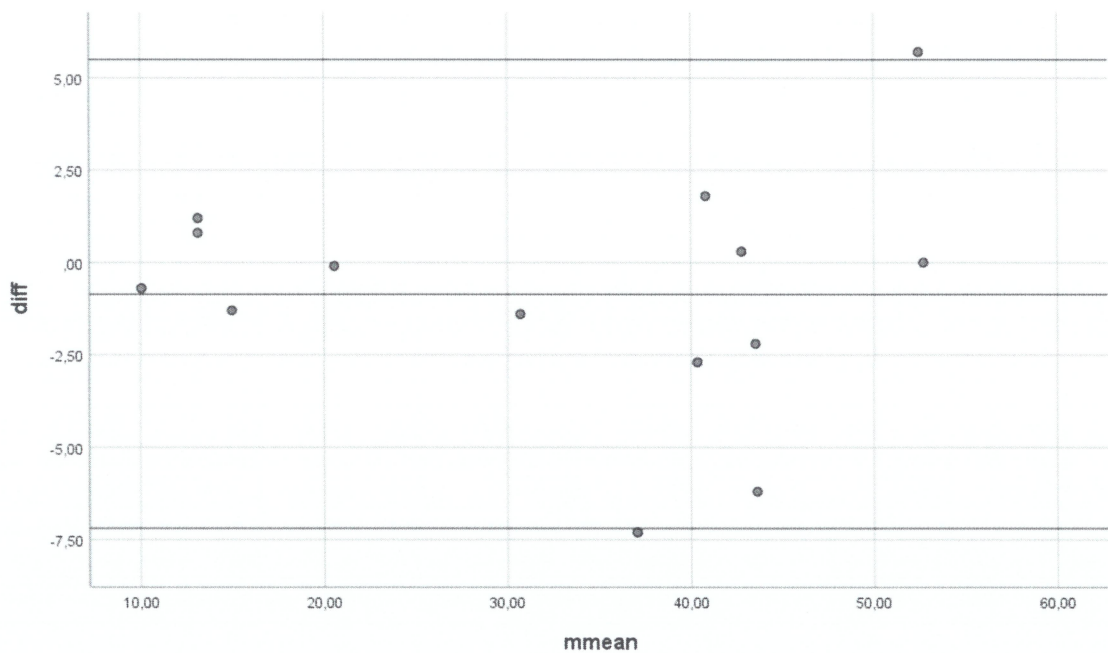


Figure 4.6. The graph of diffence and mean values in the 4.11 table and their place in the confidence interval.

In this study, we obtained ^{90}Y microsphere PET / CT images after ^{90}Y microsphere treatment and dosimetry using PM method. We defined three sections as tumor in liver, normal liver inside target and non-target normal liver. The distribution of radioactivity between tumor and normal liver is different, even if provided by the same artery. The 3-part model provides more favorable dosimetry results than a simple 2-part model that identifies only the tumor and normal liver. If we evaluate the results, %87,5 values are within the confidence interval and in this study we can show that $^{99\text{m}}\text{Tc}$ -MAA screening and activity planning based on SPECT / CT are related to post- ^{90}Y microsphere treatment dosimetry using ^{90}Y microsphere PET / CT. However, there were differences in 3 of the calculated values between the two imaging methods. It can be said that differences in calculations are thought to be due to registration errors. $^{99\text{m}}\text{Tc}$ -MAA SPECT / CT can be used as a conservative activity planning method. In addition, our study shows that ^{90}Y microsphere PET / CT is an effective method for estimating dosimetry and treatment efficacy after ^{90}Y microsphere treatment.

Although there are contradictions in the literature that $^{99\text{m}}\text{Tc}$ -MAA cannot accurately predict ^{90}Y dosimetry due to the difference in particle diameter and morphology between $^{99\text{m}}\text{Tc}$ -MAA and ^{90}Y , there are many studies that say otherwise. Our results also support that view. And it can be said that a statistically significant relationship was found between $^{99\text{m}}\text{Tc}$ -MAA SPECT/CT imaging and ^{90}Y PET / CT imaging after treatment (15,16,43).

5. CONCLUSION

The study was made to compare the mean absorbed doses of tumor, irradiated healthy parenchyma and whole liver obtained by ^{99m}Tc -MAA SPECT/CT and ^{90}Y PET / CT images before and after treatment in patients receiving ^{90}Y microsphere treatment. SPECT images were obtained by injecting an average of 185 MBq ^{99m}Tc -MAA during angiography. The required administered activities for SPECT images were calculated based on VOIs (Volume of Interests) for tumor, irradiated healthy parenchyma and whole liver using the partition method. After ^{90}Y treatment, PET / CT scan was performed and the absorbed dose was calculated with reference to ^{99m}Tc -MAA SPECT / CT images, areas for tumor, irradiated healthy parenchyma and whole liver using the same method as ^{99m}Tc -MAA SPECT. In SPECT imaging, mean tumor, irradiated healthy parenchyma and healthy liver doses were 249.7 ± 178.1 ; 93.7 ± 57.6 ; 32.1 ± 14.7 Gy, while the same values for PET / CT imaging were 247.1 ± 189.9 , 96.3 ± 60.1 ; 33.0 ± 14.8 Gy.

The absorbed dose of tumor, irradiated healthy parenchyma and whole liver calculated from PET / CT and SPECT counts were compared using Bland Altman method and 85.7% of the values were found to be within the confidence interval. In this study, it can be said that SPECT based ^{99m}Tc -MAA screening and activity planning are related to post-treatment dosimetry using ^{90}Y microsphere PET / CT. Post-treatment dosimetry based on ^{90}Y microsphere PET / CT is an effective method for predicting treatment efficacy.

Although there were differences between the dose values obtained by both imaging methods, a statistically significant relationship was found between ^{99m}Tc -MAA SPECT/CT imaging and ^{90}Y PET / CT imaging after treatment. Differences were observed in 3 patients and differences in calculations are thought to be due to registration errors.

As a result; patient-specific dosimetry should be performed. This significant relationship suggests that treatment success can be evaluated by dosimetric study after ^{90}Y PET / CT images.

6. REFERENCES

- 1) Abdel-Misih SRZ, Bloomston M. Liver Anatomy. *Surg Clin North Am.* 2010;90(4):643-653. doi:10.1016/j.suc.2010.04.017
- 2) Paulson EK. Evaluation of the Liver for Metastatic Disease. *Semin Liver Dis.* 2001;21(02):225-236. doi:10.1055/s-2001-15498
- 3) Jakobs TF, Hoffmann RT, Dehm K, et al. Hepatic yttrium-90 radioembolization of chemotherapy-refractory colorectal cancer liver metastases. *J Vasc Interv Radiol.* 2008;19:1187–1195.
- 4) Kennedy AS, Dezarn WA, McNeillie P, et al. Radioembolization for unresectable neuroendocrine hepatic metastases using resin ⁹⁰Y microspheres: early results in 148 patients. *Am J Clin Oncol.* 2008;31:271–279.
- 5) Okuda K, Ohtsuki T, Obata H, et al. Natural history of hepatocellular carcinoma and prognosis in relation to treatment study of 850 patients. *Cancer.* 1985. doi:10.1002/1097-0142(19850815)56:4<918::AID-CNCR2820560437>3.0.CO;2-E
- 6) Schafer DF, Sorrell MF. Hepatocellular carcinoma. *Lancet.* 1999.
- 7) Leong As-Y, Liew CT, Lau JWY, Johnson PJ, editors. Hepato- cellular carcinoma: contemporary diagnosis, investigation and management. *London: Arnold;* 1999.
- 8) Leung WT, Lau WY, Ho SK, et al. Measuring lung shunting in hepatocellular carcinoma with intrahepatic-arterial technetium-99m macroaggregated albumin. *J Nucl Med.* 1994.
- 9) Lambert B, Mertens J, Sturm EJ, Stienaers S, Defreyne L, D'Asseler Y. 99mTc-labelled macroaggregated albumin (MAA) scintigraphy for planning treatment with ⁹⁰Y microspheres. *Eur J Nucl Med Mol Imaging.* 2010. doi:10.1007/s00259-010-1566-2
- 10) Dawson LA, Normolle D, Balter JM, McGinn CJ, Lawrence TS, Ten Haken RK. Analysis of radiation-induced liver disease using the Lyman NTCP model. *Int J Radiat Oncol Biol Phys.* 2002. doi:10.1016/S0360-3016(02)02846-8
- 11) Salem R, Thurston KG, Carr BI, Goin JE, Geschwind J-FH. Yttrium-90 Microspheres: Radiation Therapy for Unresectable Liver Cancer. *J Vasc Interv Radiol.* 2002. doi:10.1016/S1051-0443(07)61790-4

- 12) Salem R, Thurston KG. Radioembolization with yttrium-90 microspheres: A state-of-the-art brachytherapy treatment for primary and secondary liver malignancies - Part 3: Comprehensive literature review and future direction. *J Vasc Interv Radiol*. 2006. doi:10.1097/01.RVI.0000236744.34720.73
- 13) Gulec SA, Mesoloras G, Stabin M. Dosimetric techniques in ⁹⁰Y microsphere therapy of liver cancer: The MIRD equations for dose calculations. *J Nucl Med*. 2006.
- 14) Emami B, Lyman J, Brown A, et al. Tolerance of normal tissue to therapeutic irradiation. *Int J Radiat Oncol Biol Phys*. 1991. doi:10.1016/0360-3016(91)90171-Y
- 15) Fabbri C, Sarti G, Agostini M, et al. SPECT/CT ⁹⁰Y-Bremsstrahlung images for dosimetry during therapy. *Ecancermedicalscience*. 2008;2:106.
- 16) D'Arienzo M, Chiaramida P, Chiacchiararelli L, et al. ⁹⁰Y PETbased dosimetry after selective internal radiotherapy treatments. *Nucl Med Commun*. 2012;33:633–640.
- 17) Chiesa C, Maccauro M, Romito R, et al. Need, feasibility and convenience of dosimetric treatment planning in liver selective internal radiation therapy with ⁹⁰Y microspheres: The experience of the National Cancer Institute of Milan. *Q J Nucl Med Mol Imaging*. 2011.
- 18) Strigari L, Sciuto R, Rea S, et al. Efficacy and Toxicity Related to Treatment of Hepatocellular Carcinoma with ⁹⁰Y-SIR Spheres: Radiobiologic Considerations. *J Nucl Med*. 2010. doi:10.2967/jnumed.110.075861
- 19) Cherry S, Sorenson J, Phelps M. *Physics in Nuclear Medicine*.; 2012. doi:10.1016/C2009-0-51635-2
- 20) Westcott MA, Coldwell DM, Liu DM, Zikria JF. The development, commercialization, and clinical context of yttrium-90 radiolabeled resin and glass microspheres. *Adv Radiat Oncol*. 2016;1(4):351-364. doi:10.1016/j.adro.2016.08.003
- 21) Enghag P. Scandium, Yttrium, Lanthanum and the 14 Lanthanides– Rare Earth Metals (REMs). In: *Encyclopedia of the Elements*. ; 2008. doi:10.1002/9783527612338.ch17
- 22) Walker LA. Radioactive yttrium 90: A review of its properties, biological behavior, and clinical uses. *Acta Radiol*. 1964;2:302- 314.

- 23) D'Arienzo M. Emission of β^+ Particles Via Internal Pair Production in the $0^+ - 0^+$ Transition of ^{90}Zr : Historical Background and Current Applications in Nuclear Medicine Imaging. *Atoms*. 2013. doi:10.3390/atoms1010002
- 24) Simon N, Feitelberg S. Scanning Bremsstrahlung of Yttrium-90 Microspheres Injected Intra-arterially. *Radiology*. 2014. doi:10.1148/88.4.719
- 25) Minarik D, Sjögren Gleisner K, Ljungberg M. Evaluation of quantitative ^{90}Y SPECT based on experimental phantom studies. *Phys Med Biol*. 2008. doi:10.1088/0031-9155/53/20/008
- 26) Elschot M, Vermolen BJ, Lam MGEH, de Keizer B, van den Bosch MAAJ, de Jong HWAM. Quantitative Comparison of PET and Bremsstrahlung SPECT for Imaging the In Vivo Yttrium-90 Microsphere Distribution after Liver Radioembolization. *PLoS One*. 2013. doi:10.1371/journal.pone.0055742
- 27) Ehrhardt GJ, Day DE. Therapeutic use of ^{90}Y microspheres. *Int J Rad Appl Instrum B*. 1987;14:233-242
- 28) Burrill J, Hafeli U, Liu DM. Advances in radioembolization - Embolics and isotopes. *Nuclear Medi Radiat Ther*. 2011;2:107.
- 29) TheraSphere Yttrium-90 Microspheres Package Insert, v12 Surrey, UK: Biocompatibles UK Ltd. Available at: https://www.btgim.com/getattachment/Therasphere/US/Products/Indications/TheraSphere-Package-Insert_USA_v13.pdf.aspx.
- 30) Lewandowski RJ, Minocha J, Memon K, et al. Sustained safety and efficacy of extended-shelf-life (^{90}Y) glass microspheres: longterm follow-up in a 134-patient cohort. *Eur J Nucl Med Mol Imaging*. 2014;41:486-493.
- 31) Westcott MA, Coldwell DM, Liu DM, Zikria JF. The development, commercialization, and clinical context of yttrium-90 radiolabeled resin and glass microspheres. *Adv Radiat Oncol*. 2016;1(4):351-364. doi:10.1016/j.adro.2016.08.003
- 32) Kao YH, Tan EH, Ng CE, Goh SW. Clinical implications of the body surface area method versus partition model dosimetry for yttrium-90 radioembolization using resin microspheres: A technical review. *Ann Nucl Med*. 2011;25(7):455-461. doi:10.1007/s12149-011-0499-6

- 33) Lau WY, Kennedy AS, Kim YH, et al. Patient selection and activity planning guide for selective internal radiotherapy with yttrium-90 resin microspheres. *Int J Radiat Oncol Biol Phys.* 2012;82:401–407.
- 34) Lawrence TS, Robertson JM, Anscher MS, et al. Hepatic toxicity resulting from cancer treatment. *Int J Radiat Oncol Biol Phys.* 1995;31:1237–1248.
- 35) Salem R, Lewandowski RJ, Sato KT, et al. Technical aspects of radioembolization with 90Y microspheres. *Tech Vasc Interv Radiol.* 2007;10:12–29
- 36) Giavarina D. *Bm-25-141.* 2015;25(2):141-151. doi:10.11613/BM.2015.015
- 37) Ljungberg M, Sjögren Gleisner K. Personalized Dosimetry for Radionuclide Therapy Using Molecular Imaging Tools. *Biomedicines.* 2016. doi:10.3390/biomedicines4040025
- 38) Kennedy A, Coldwell D, Sangro B, et al. Radioembolization for the treatment of liver tumors general principles. *Am J Clin Oncol.* 2012;35:91–99.
- 39) Sangro B, Salem R, Kennedy A, et al. Radioembolization for hepatocellular carcinoma: a review of the evidence and treatment recommendations. *Am J Clin Oncol.* 2011;34:422–431.
- 40) Murthy R, Kamat P, Nunez R, et al. Radioembolization of yttrium- 90 microspheres for hepatic malignancy. *Semin Intervent Radiol.* 2008;25:48–57.
- 41) Carr BI. Hepatic arterial 90Yttrium glass microspheres (Therasphere) for unresectable hepatocellular carcinoma: interim safety and survival data on 65 patients. *Liver Transpl.* 2004;10(2 Suppl 1):S107– S110.
- 42) Dancey JE, Shepherd FA, Paul K, et al. Treatment of nonresectable hepatocellular carcinoma with intrahepatic 90Y-microspheres. *J Nucl Med.* 2000;41:1673–1681.
- 43) Wondergem M, Smits ML, Elschot M, et al. 99mTc-macroaggregated albumin poorly predicts the intrahepatic distribution of 90Y resin microspheres in hepatic radioembolization. *J Nucl Med.* 2013;54:1294–1301.
- 44) Khalil MM. *Basic Sciences of Nuclear Medicine.*; 2011. doi:10.1007/978-3-540-85962-8
- 45) Mir DIA, Risk BB, Cronan J, et al. Defining the relationship between radiation dose, tumor response and associated liver toxicity in hepatocellular

carcinoma after Y90 radioembolization: a systematic review and meta-analysis. *Abstract 116. Society of Interventional Radiology meeting.*
Presented on March 24, 2019.

7. ETHICS COMMITTEE REPORT



T.C. YEDİTEPE ÜNİVERSİTESİ

Sayı : 37068608-6100-15-1323
Konu: Klinik Araştırmalar
Etik kurul Başvurusu hk.

13/04/2017

İlgili Makama (Nalan Alan Selçuk)

Yeditepe Üniversitesi Hastanesi Nükleer Tıp Anabilim Dalı Doç. Dr. Nalan Alan Selçuk'un sorumlu olduğu "**Selektif İntraarteriyel Radyonüklid Tedavide Tümör Dozu-Cevap İlişkisinin Retrospektif Değerlendirilmesi**" isimli araştırma projesine ait Klinik Araştırmalar Etik Kurulu (KAEK) Başvuru Dosyası (1313 kayıt Numaralı KAEK Başvuru Dosyası), Yeditepe Üniversitesi Klinik Araştırmalar Etik Kurulu tarafından 12.04.2017 tarihli toplantıda incelenmiştir.

Kurul tarafından yapılan inceleme sonucu, yukarıdaki isimi belirtilen çalışmanın yapılmasının etik ve bilimsel açıdan uygun olduğuna karar verilmiştir (KAEK Karar No: 707).

Prof. Dr. Turgay ÇELİK
Yeditepe Üniversitesi
Klinik Araştırmalar Etik Kurulu Başkanı

8. CV

Kişisel Bilgiler

Adı	Gamze	Soyadı	Ergiyen Buldu
Doğum Yeri	Bornova	Doğum Tarihi	03.06.1988
Uyruğu	TC	TC Kimlik No	14810639046
E-mail	gamzeergiyen@hotmail.com	Tel	0537 482 21 73

Öğrenim Durumu

Derece	Alan	Mezun Olduğu Kurumun Adı	Mezuniyet Yılı
Doktora			
Yüksek Lisans			
Lisans	Fizik	Yeditepe Üniversitesi	2013
Lise	Fen	İzmir Anadolu Lisesi	2006

Bildiği Yabancı Dilleri	Yabancı Dil Sınav Notu (#)

Başarılmış birden fazla sınav varsa (KPDS, ÜDS, TOEFL; EELTS vs), tüm sonuçlar yazılmalıdır

İş Deneyimi (Sondan geçmişe doğru sıralayın)

Görevi	Kurum	Süre (Yıl - Yıl)
Lisansüstü Bursiyer	Yeditepe Üni.	1,5
Lab. Müdür Yardımcısı	Protos Kalibrasyonu	3,5

Bilgisayar Bilgisi

Program	Kullanma becerisi
Excel, word, powerpoint	Çok iyi

*Çok iyi, iyi, orta, zayıf olarak değerlendirin

Bilimsel Çalışmaları

SCI, SSCI, AHCI indekslerine giren dergilerde yayınlanan makaleler

Diğer dergilerde yayımlanan makaleler

Uluslararası bilimsel toplantılarda sunulan ve bildiri kitabında (*Proceedings*) basılan bildiriler

Hakemli konferans/sempozyumların bildiri kitaplarında yer alan yayımlar

Diğer (Görev Aldığı Projeler/Sertifikaları/Ödülleri)
